Cost Reduction of School Bus Fleet Electrification With Optimized Charging and Distributed Energy Resources

Preprint

William Becker, Eric Miller, Partha Pratim Mishra, Rishabh Jain, Dan Olis and Xiangkun Li

National Renewable Energy Laboratory

Presented at the 2019 North American Power Symposium
Wichita, Kansas
October 13–15, 2019

NREL is a national laboratory of the U.S. Department of Energy
Office of Energy Efficiency & Renewable Energy
Operated by the Alliance for Sustainable Energy, LLC

This report is available at no cost from the National Renewable Energy Laboratory (NREL) at www.nrel.gov/publications.

Contract No. DE-AC36-08GO28308

Conference Paper
NREL/CP-7A40-74187
March 2020

Cost Reduction of School Bus Fleet Electrification With Optimized Charging and Distributed Energy Resources

Preprint

William Becker, Eric Miller, Partha Pratim Mishra, Rishabh Jain, Dan Olis and Xiangkun Li

National Renewable Energy Laboratory

Suggested Citation
Becker, William, Eric Miller, Partha Pratim Mishra, Rishabh Jain, Dan Olis and Xiangkun Li. 2020. *Cost Reduction of School Bus Fleet Electrification With Optimized Charging and Distributed Energy Resources: Preprint*. Golden, CO: National Renewable Energy Laboratory. NREL/ CP-7A40-74187. https://www.nrel.gov/docs/fy20osti/74187.pdf

NREL is a national laboratory of the U.S. Department of Energy
Office of Energy Efficiency & Renewable Energy
Operated by the Alliance for Sustainable Energy, LLC

This report is available at no cost from the National Renewable Energy Laboratory (NREL) at www.nrel.gov/publications.

Contract No. DE-AC36-08GO28308

Conference Paper
NREL/CP-7A40-74187
March 2020

National Renewable Energy Laboratory
15013 Denver West Parkway
Golden, CO 80401
303-275-3000 • www.nrel.gov

NOTICE

This work was authored by the National Renewable Energy Laboratory, operated by Alliance for Sustainable Energy, LLC, for the U.S. Department of Energy (DOE) under Contract No. DE-AC36-08GO28308. Funding provided by the U.S. Department of Energy Office of Energy Efficiency and Renewable Energy and Eaton Corporation.. The views expressed herein do not necessarily represent the views of the DOE or the U.S. Government. The U.S. Government retains and the publisher, by accepting the article for publication, acknowledges that the U.S. Government retains a nonexclusive, paid-up, irrevocable, worldwide license to publish or reproduce the published form of this work, or allow others to do so, for U.S. Government purposes.

Cover Photos by Dennis Schroeder: (clockwise, left to right) NREL 51934, NREL 45897, NREL 42160, NREL 45891, NREL 48097, NREL 46526.

Cost Reduction of School Bus Fleet Electrification With Optimized Charging and Distributed Energy Resources

William Becker
National Renewable Energy Laboratory
Golden, Colorado
Email: William.Becker@nrel.gov

Eric Miller
National Renewable Energy Laboratory
Golden, Colorado
Email: Eric.Miller@nrel.gov

Partha Pratim Mishra
National Renewable Energy Laboratory
Golden, Colorado
Email: Partha.Mishra@nrel.gov

Rishabh Jain
National Renewable Energy Laboratory
Golden, Colorado
Email: Rishabh.Jain@nrel.gov

Dan Olis
National Renewable Energy Laboratory
Golden, Colorado
Email: Dan.Olis@nrel.gov

Xiangkun Li
National Renewable Energy Laboratory
Golden, Colorado
Email: Xiangkun.Li@nrel.gov

***Abstract*—Considerations for electrifying school buses are presented with an analysis of battery sizing to match bus-driving requirements. The charging and vehicle-to-building dispatch of the electric school buses were optimized to evaluate the potential to reduce the impact of the bus charging on the school's electric utility bill. Distributed energy resources and flexible building loads were also considered with the school bus electrification to evaluate the further reductions in energy costs with enhanced systems integration and optimized dispatch. The effect of degradation on the school bus batteries was analyzed to determine if the smart-charging and vehicle-to-building battery operation decreases the life of the battery. The results show that there is an opportunity to mitigate the increase in electric utility bill with improved charging controls and bi-directionally operating the school bus batteries. The battery degradation analysis using dispatch with optimized charging and discharging shows that acceptable battery life remains.**

Keywords*—*Electric Vehicle, School Bus, Fleet Electrification, Distributed Energy Resources, smart-charging, Vehicle-To-Grid.

I. Introduction

The electrification of medium- and heavy-duty vehicles has numerous societal benefits. When compared to their diesel counterparts, electric vehicles (EVs) are quieter, reduce combustion product emissions to zero, and are mechanically simpler, making them easier to maintain. Diesel school buses have been shown to increase the exposure of school children to aerosol pollutants including diesel exhaust particulates [1]. Exposure to these particulates is linked to weezing and decreased lung function [2]. Additionally, reduced maintenance needs benefits school districts, which often lack the infrastructure to make major repairs to their fleets.

Although the electrification of vehicles provides savings by eliminating diesel fuel and reducing maintenance costs, the electricity required for charging is an added cost. Commercial scale buildings such as schools typically have utility rates that include both energy and demand charges (potentially dependent on the time of use). If charging occurs during peak electric rate times, this energy can be expensive. If charging coincides with the peak building loads, increased demand charges are incurred. There is an opportunity to reduce energy and demand charges by implementing smart-charging controls and by integrating distributed energy resources (DERs) along with vehicle electrification.

REopt™ is a techno-economic optimization model developed by the National Renewable Energy Laboratory (NREL). It is a planning tool formulated as a mixed-integer linear program to optimally size and dispatch the DERs and storage-based assets given the historical building loads and rate tariffs for a specific site [3]. The range of loads, technology resources, drivers, and outputs considered in the model are shown in Fig. 1. The most common objective function of the model is to minimize the life-cycle cost (LCC) of energy. In this work, solar photovoltaics (PV), stationary battery, and chilled water tank thermal energy storage (TES) technologies are modeled. The addition of the electric school bus fleet into the REopt model is a key innovation of this work that enables an integrated optimization of DER technologies and smart-charging EV batteries to minimize life-cycle energy costs.

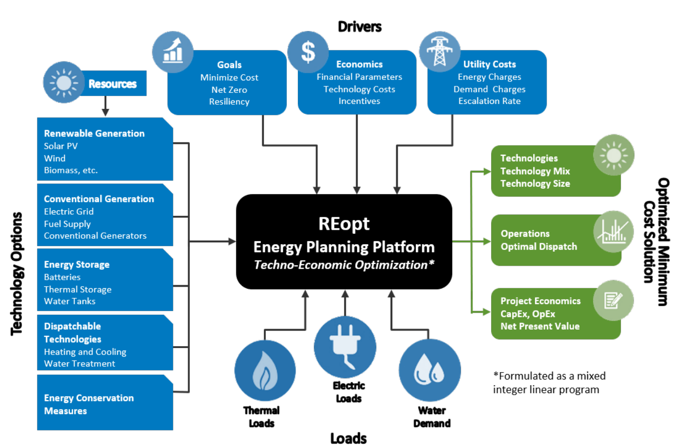

Fig. 1: REopt techno-economic optimization tool. Source: [3]

In any EV application, it is important to understand how long the batteries will last given the specific usage scenario because batteries are by far the costliest component in an EV [4]. Significant advances have been made on lithium-ion (Li-ion) battery life-degradation modeling and analysis with the underlying literature spanning research topics from understanding battery-aging mechanisms [5] to developing mathematical models for health-conscious control applications [6]. In this paper, one objective is to analyze the impact on the long-term health of the EV batteries from controlling and dispatching them in ways to reduce the school's electric utility bill.

The case study presented is a school in New Jersey. Various scenarios are analyzed as illustrated in Fig. 2. The analysis assumes that buses are parked at the school when they are not driving. While buses are often parked at depots for fueling and maintenance, the results of this analysis show that there may be an economic incentive to park EV buses at schools so that they can be used to manage utility bills and potentially contribute to resilience. Scenario 1 represents the business as usual case, where the school purchases all electricity from the utility, and uses diesel buses. Scenario 2 considers opportunities for utility bill reduction through DERs, but still uses diesel buses. In Scenario 3, six electric buses are introduced with a manual charging strategy of charging the buses as soon as they return back to the school. Scenario 4 allows REopt to optimally charge the buses (while still meeting the charge requirement for driving) to mitigate excess energy and demand charge costs. In scenarios 5 and 6, REopt optimally sizes DER technologies under manual (5) and smart-charging (6) scenarios for the electric buses. Scenario 7 assumes the buses are able to discharge the battery energy back to the building load, which is referred to in this paper as "vehicle to building" (VTB), in order to further reduce energy and demand charges.

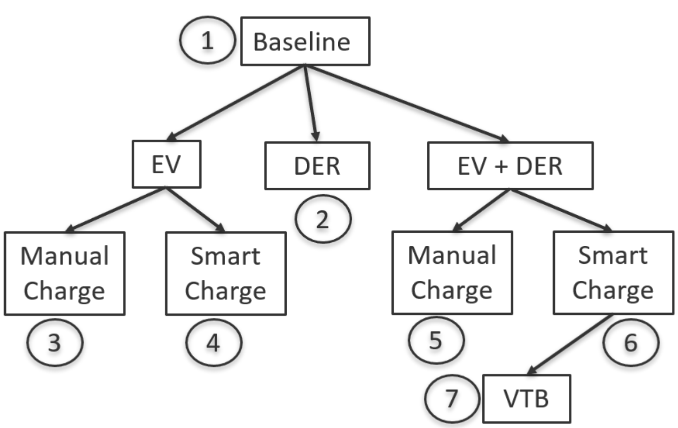

Fig. 2: Scenarios of electrification and DER technologies analyzed.

II. METHODS

The duty cycles of the electric school buses were simulated using an electric school bus model and data logged from school buses used in Torrance, California; although not geographically similar to New Jersey, this was the best available data and the school bus driving profiles are representative of a suburban school anywhere in the United States. The GPS coordinates and elevation of each bus were logged every second. From these measures, vehicle speed, acceleration, and road grade were calculated. The vehicle drivetrain model is a variant of NREL's FastSim vehicle simulation tool [7]. This type of model is called backward-looking, because it uses recorded driving profiles to calculate the energy expenditure of the vehicle working backward through the drivetrain. The benefit of these models is that the they do not involve any iteration, making them faster to execute. The drivetrain model is described in (1), and further in [1], with vehicle parameters listed in Table I:

TABLE I: Drivetrain Model Parameters

Symbol	Value	Units	Description
m	15195	kg	Vehicle mass
C_{rr}	0.008	-	Rolling resistance coefficient
C_{dl}	3.8	$\frac{N}{(m/s)^2}$	Drag coefficient
r_{tr}	4.5/1.0	-	Transmission gearing (2-speed)
η_{tr}	0.98	-	Transmission efficiency
r_{df}	4.5	-	Differential gearing
η_{df}	1	-	Differential efficiency

$$\begin{aligned}
\xrightarrow[v]{\theta} F &= m\frac{dv}{dt} + mgsin(\theta) + mgC_{rr}cos(\theta) + C_{dl}v^2 \\
\xrightarrow[v]{F} \tau_{df} &= \frac{Fr_{wheel}}{\eta_{df}r_{df}},\ \omega_{df} = \frac{vr_{df}}{r_{wheel}} \\
\xrightarrow[\omega_{df}]{\tau_{df}} \tau_{tr} &= \frac{\tau_{df}}{\eta_{tr}r_{tr}},\ \omega_{tr} = \omega_{df}r_{tr} \\
\xrightarrow[\omega_{tr}]{\tau_{tr}} P_{em} &= \frac{\tau_{tr}\omega_{tr}}{\eta_{em}(\omega_{tr},\tau_{tr})} \\
\xrightarrow{P_{em}} E_{es} &= E_{es} - P_{em}\Delta t
\end{aligned} \tag{1}$$

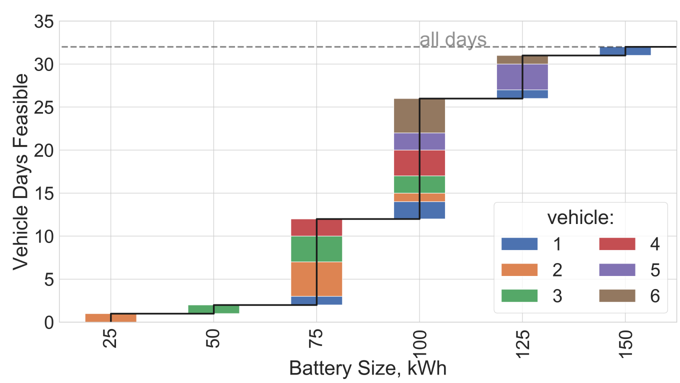

Fig. 3: Battery sizing by daily energy use.

In order to replace 100% of the diesel buses with electric buses, it is important that the buses have sufficient battery capacity. Using the model described above, the daily energy use of each bus for each day of one week was estimated. Average consumption was $1.58\frac{kWh}{mi}$ and $\frac{76}{k}Wh/day$. The battery size needed to complete a day of operation is estimated by multiplying the daily energy consumption by a factor of safety of 1.25 and rounding to the nearest 25 kWh increment. Figure 3 shows that 31 of 32 vehicle days simulated could be completed with a battery size of 125 kWh. It also shows that buses 2,3, and 4 could complete complete their daily driving with a 100 kWh battery. In practice, fleet electrification

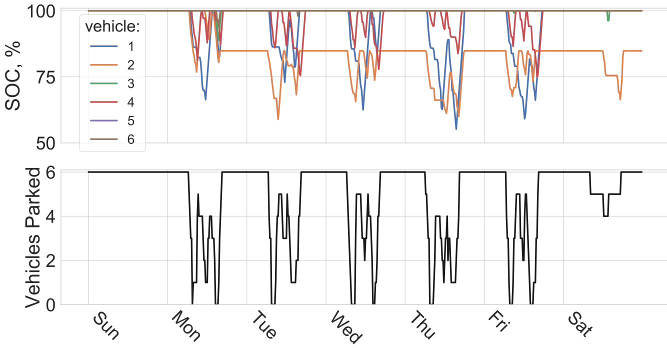

Fig. 4: State of charge and occupancy of bus depot for a week

can be a gradual process, using EVs on shorter routes, and gradually replacing conventional vehicles which drive progressively more energy-intense schedules. To be conservative in battery sizing, a battery capacity of 150 kWh was chosen for each bus to ensure that 100% of the vehicle days could be replaced with electric driving this battery also allows each bus to drive for an entire day without recharging. In-use, school buses have the opportunity to charge in the middle of the day while school is in session. To evaluate these opportunities, a geofence was drawn around the central bus depot. Figure 4 shows the number of buses parked and eligible for charging by time of day. On weekdays, the buses were parked for an average of $3.02\frac{hr}{day}$ between the hours of 8AM and 2PM. When the vehicles are able to charge during the day in addition to charging in the evening, their depth of discharge (DOD) never drops below 50% SOC. Downsizing batteries by leveraging charging opportunities significantly reduces the capital cost of an EV, currently by about $500/kWh.

Typically, buses are plugged in to start charging as soon as the buses return to the school, and this is the case for the Manual Charging scenarios. Figure 5 shows an example week of school electric load with the added load from bus charging in the manual charging scenarios, and it shows that the charging load is mostly additive to the peak school load which will increase demand charges.

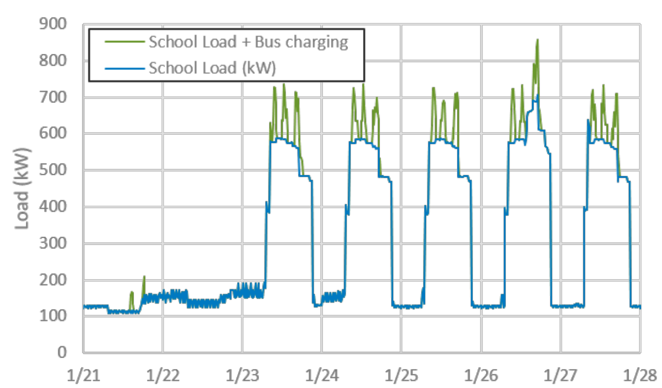

Fig. 5: Example week of manual bus charging added to school load.

For smart-charging and VTB scenarios, an optimization capability is needed. The addition of the EV fleet (school buses) to REopt is a new innovation from this work. The driving energy required for the N vehicles (six in this case) is now an input to REopt and a new constraint is added to ensure that the bus battery minimum state of charge requirement is achieved at the time that the bus leaves the school. For smart-charging, REopt is allowed to optimize when the vehicle charges so long as it still meets the minimum state of charge requirement prior to the trip. For VTB, REopt is allowed to discharge energy from the bus battery when it is docked at the charging station while the charge requirements for each driving route are still met.

The school electric loads are generated using the DOE commercial Reference Buildings [8] using the following location: Baltimore, Maryland, ASHRAE 90.1-2004 (nearest location to New Jersey with the same climate zone). The year-long hourly load profile has a minimum, maximum, and average load of 96, 1189, and 367 kW respectively with a total energy consumption of 3,218,300 kWh over the year.

The energy and demand charges assumed in the analysis are based on the local utility and independent system operator (ISO) charges. The utility rate structure is from Orange and Rockland Utilities, Rockland Electric Company (RECO), General Service, No. 2 Service Class with Basic Generation Service. The tariff details are shown in Table II [9]. The energy rate is based on utility distribution charges plus the hourly-varying PJM real-time price signal for the Rockland Electric Transmission Zone. Demand charges are quite low, but there is an additional demand-like charge within the PJM operating territory called "Peak Load Contribution" (PLC, also known as coincident peak and 5CP). This charge is based on the customer's load during the PJM system's five highest load-hours, which typically occur in the summer.

TABLE II: Electric Utility Rate Structure Used in the Case Study

	Value	Units
Energy Charges Summer/Winter[a]	0.07049/0.0672	$/kWh
Energy Adder of PJM Real Time Market Price[b]	Varies by Hour	$/kWh
RECO Demand Charges Summer/Winter[a]	1.51/1.27	$/kW-month
PJM Peak Load Contribution	9.76	$/kW-month

[a] Summer includes June, July, August, and September
[b] Average PJM Real Time Price in 2018 was $0.029/kWh

Although an uninformed building energy manager may not know when these peak hours occur, there are companies for-hire that act as a curtailment service provider (CSP) and can predict system peak hours and inform the school to reduce load (or dispatch a battery, for example). To account for uncertainty in predicting the exact peak load hours, CSPs will typically tell customers to reduce load across a larger number of hours, to increase the probability of reducing load during the 5 peak hours. For this analysis, we modeled the 32 highest PJM system load hours and the building's PLC was calculated as the average of the school's load during those hours.

There are four options for REopt to use available assets to reduce load, but their availability depends on the scenario considered:

1) Avoid EV charging (only available in smart-charging scenarios)

2) Use stored chilled water to reduce the electric chiller load
3) Discharge a stationary battery (if chosen)
4) Discharge the EV battery (only available in VTB scenario)

Table III shows the life cycle economic analysis inputs used in the case study.

TABLE III: Life Cycle Economic Analysis Inputs

Objective	Minimize life-cycle cost
Ownership models	Direct purchase
Analysis period	25 years
Discount rate (nominal)	3%
General inflation rate	1%
Electricity cost escalation rate (nominal)	2%/yr
Interconnection limit	Unlimited
Net metering limit	Not to exceed annual site load

Table IV shows the DER technology cost and performance characteristics assumed for the analysis. The estimated rooftop area available for PV limits the PV size to 500 kW-DC, so that is set as a maximum size in REopt.

TABLE IV: Distributed Energy Resource Technology Characteristics

Solar PV	
PV array type	Rooftop
Space available for PV	500-kW-DC max
Total installed costs	\$1.708/W-DC
Annual O&M costs	\$16/kW-DC
Technology resource	TMY3 solar in Montvale, NJ
Stationary Battery Storage	
Battery chemistry	Lithium-ion
Capital costs	\$1000/kW + \$500/kWh
Replacement	Year 10
Replacement costs	\$460/kW + \$230/kWh
AC-AC round-trip efficiency	89.9%
Minimum state of charge	20%
Thermal Energy Storage	
Type	Single chilled water tank
Capital costs	\$2/gal
Approximate daily figure-of-merit	85%90%
Minimum state of charge	10%

The battery life degradation analysis framework developed by NREL is used to rapidly investigate the extent to which specific battery usage profiles degrade the life of the battery by reducing its usable capacity [10]. This framework uses simple proxy rate models, whose parameters are identified through model regression of rapid-aging experimental data, to reflect a decrease in usable capacity of the battery and increase in internal resistance. An example of a capacity-fade model and fade-rate model from this framework is shown in (2) [11]:

$$
\begin{aligned}
&Q_{Li} = b_0 - b_1 t_{life}^{1/2}, \quad Q_{sites} = c_0 - c_2 N \\
&b_1 = \frac{b_{1,ref}}{\Delta t_{cyc}} \int_{t_{cyc}} \Big[exp\big(-\frac{E_a}{R}(1/T - 1/T_{ref})\big) \times \\
&\quad exp\big(-\frac{\alpha F}{R}(U_{neg}/T - U_{neg,ref}/T_{ref})\big) \times \\
&\quad exp\big(\mu_{b_1} \frac{max(\Delta DOD)^{\beta_{b_1}}}{\Delta DOD_{ref}}\big)\Big]
\end{aligned} \tag{2}
$$

where Q_{Li} and Q_{sites} represent the remaining capacity after cyclable Li-ion loss (resulting from solid-electrolyte interface growth from calendar time, t_{life}, and cycling) and active site loss (due to mechanical damage to the electrodes from cycling). The model parameters (b_0, c_0, $b_{1,ref}$, E_a, etc.) are identified from aging data regression. The parametric structure of these models is rooted in physics-based justifications such as the dependence of the fade rate, b_1, on temperature through an Arrhenius relationship (i.e. $exp\big(-\frac{E_a}{R}(1/T - 1/T_{ref})\big)$). For a comprehensive discussion on battery life models and parameterization, see [10], [11]. We use five different battery technology life models developed using this framework to analyze capacity degradation based on the REopt cycling profiles. REopt's dispatches are not informed by degradation functions and therefore are battery technology agnostic. Different technologies have been known to show different aging behaviors for the same operating conditions. Thus, we post-process the REopt dispatches to perform degradation analysis in this paper by: (1) selecting a representative battery cycling profile (defined by time-series data of input current or power, corresponding state-of-charge (SOC), and temperature of the battery cell); (2) selecting a battery model (four battery technologies spanning three chemistries, namely: lithium nickel cobalt aluminum oxide (NCA), lithium nickel manganese cobalt oxide (NMC), and lithium iron phosphate (LFP)); and (3) simulating the life model for 10 service years and identifying how the capacity decays and which stress factors (temperature, SOC, depth-of-discharge etc.) contribute primarily to capacity fade.

The REopt optimization model is used with the input data described above to minimize life cycle cost of energy. The scenarios are compared to understand the value of implementing smart controls and integrating DERs with the EV bus fleet.

III. Results

The life cycle cost analysis results for the seven scenarios are shown in Fig. 6 and Table V. In addition to electric utility cost differences, the diesel fuel cost savings from electrification are quantified. The school bus energy determined by the vehicle drive-train model is converted to diesel fuel consumption. The avoided annual diesel fuel consumption for all size buses is calculated to be 7,274 gallons. The levelized cost of diesel fuel is estimated to be \$3.86/gal (current diesel price of \$3.32/gal escalated by 0.6%/year); this amounts to an annualized savings of \$28.1K/year and a life cycle cost savings of \$489.3K.

These results do not explicitly include an estimate for the capital cost of the EV buses and the charging and controls equipment, and they also do not include maintenance cost savings from EVs. The net present value (NPV) of scenarios 3-7 therefore represent the capital cost less any maintenance cost savings that could be paid to make the project break-even. The available capital cost to be spent on the EV bus and charging equipment and controls at the break-even point is shown in the last row of Table V. Note, that any maintenance cost savings from EVs would add to the break-even cost per bus.

Scenario 1 is the business-as-usual case, and shows the life cycle cost of energy to the school if they make no changes, and continue to purchase all of their energy from the utility and run diesel buses. The life cycle cost of all other scenarios is compared to Scenario 1 to identify whether the school saves money or loses money by making a change. Scenario 2 (DER only) shows that the school can save almost \$1M in life cycle energy costs by investing in DER (PV and TES) while continuing to run diesel buses. For all scenarios which consider DER, REopt selected the maximum PV size of 500 kW-DC.

Adding EVs without DER results in a slightly positive NPV, but this is assumed to be too low of a break-even cost to pay for buses and infrastructure with only \$37K available for the manual charging (scenario 3) and \$48K available for smart charging (scenario 4).

By combining DER with the EVs, the savings provided by DER can be used to offset the costs of the EVs, resulting in a break-even cost per bus of greater than \$200K from which to purchase the EV buses and charging infrastructure. This is believed to be adequate to pay for the incremental cost of EV buses (replacing diesel buses) and charging infrastructure based on an NREL estimate of these costs. DER with EV manual charging (scenario 5) has a break-even cost of \$201K, and DER with smart-charging improves this slightly to \$211K. However, the biggest benefit in EV control comes from using EV batteries to help reduce building peak load and perform energy arbitrage (scenario 7); this scenario increases the break-even cost by greater than 20% to \$256K when compared to DER with smart-charging EVs. It should be noted that VTB will require greater controls and equipment functionality which comes at an additional cost.

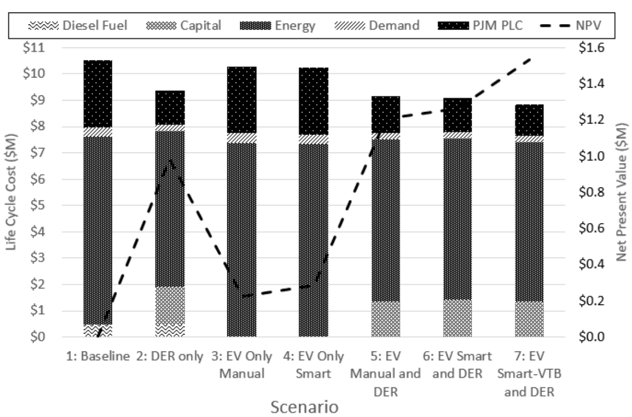

Fig. 6: Life cycle cost results for all scenarios.

Table V quantifies the economic benefits of all the electrification scenarios, establishing that EV smart-charging with VTB and DER (Scenario 7) is the most profitable one in the case studies considered in this paper. To compare Scenario 7 to a baseline vehicle usage case (no REopt based optimization) viś-a-viś the life of the battery, we use the life models for four battery technologies: a 50 Ah NCA cell, a 15 Ah NMC cell (NMC #1), a 20 Ah LFP cell, and a 25 Ah NMC cell (NMC #2). It is assumed that the cell temperature is the same as the ambient temperature[1] [12]. Fig. 7 shows the capacity-degradation trends for the four battery technologies when subjected to the cycling profile of Scenario 7 and a non-optimized baseline case. Except for the LFP technology, the other technologies show remaining capacities of 80% or higher after 10 years of operation under the REopt-based cycling. Such longevity of the battery technologies can be attributed to: (a) less cycling by REopt's optimal dispatch strategy (input power is zero for >80% of the cycling time) and (b) an average SOC closer to the mid SOC range throughout the cycling period (∼53%). Milder ambient temperature conditions of New Jersey (mean temperature of ∼13°C) is also contributing to the slower capacity degradation seen in Fig. 7a. The baseline case shows less capacity degradation for NMC #1 and NMC #2 compared to Scenario 7 but more degradation for NCA and LFP. This is owing to the contrasting SOC and DOD characteristics of the baseline case and Scenario 7. For instance, lower average SOC (53% vs 97%) of Scenario 7 helps NCA and LFP models to exhibit lesser degradation compared to baseline. However, higher maximum DOD (85% vs 41%) of Scenario 7 makes NMC #1 and NMC #2 to degrade more compared to baseline. To understand the impact of temperature variation on battery life, we subject the battery technologies to the same cycling profile but with different thermal conditions, namely constant temperatures of 0°C and 36°C. Fig. 7b shows that a higher temperature can significantly decrease the life of a Li-ion battery. For example, after 10 years at 36°C, the capacity of NMC #1 decays completely to 0% and the capacities of the other technologies decrease to 50% or lower of the initial capacity. However, at 0°C, capacity decay is slowed compared to the ambient temperature case. This is specific to the usage profile of the applications considered in this paper. At such low temperature, capacity degradation slows down when the battery is kept in storage (i.e. no load condition). In scenario 7, more than 80% of the time, the input power to the EV battery is zero, which results in slower capacity fade at 0°C.

[1]In practice, a well-calibrated thermal model would predict the temperature of the cell with the ambient temperature being an external input signal to the model

IV. Conclusions

The life cycle cost of energy impacts of electrifying school buses under various scenarios is presented. By combining DER with the EVs, the savings provided by DER can be used to offset the electric charging costs of the EVs, resulting in a break-even cost per bus of greater than \$200K which is estimated to be sufficient to purchase the EV buses and charging infrastructure. Improved controls which can provide intelligent charging strategies can mitigate the impact of EV charging on energy and demand costs. With additional hardware and controls functionality, enabling the EVs to discharge to offset building load reduces demand and energy charges and provides a net utility bill cost reduction when including DERs such as PV and flexible building loads enabled by chilled water thermal energy storage. Furthermore, battery life analysis results indicate that electrified school buses can participate in VTB activities for net cost reduction without sacrificing battery life significantly. However, proper thermal management is important to maintain battery life.

V. Future Work

Future work will explore additional revenue stream opportunities of the EVs by considering demand response and wholesale market participation in different regions of the United States. Other cost considerations to be investigated

TABLE V: Life Cycle Analysis Results for All Scenarios

	1: Business-as-usual	2: DER only	3: EV Only Manual	4: EV Only Smart	5: EV Manual and DER	6: EV Smart and DER	7: EV Smart-VTB and DER	Units
PV Size	-	500	-	-	500	500	500	kW-DC
TES Size	-	2,286	-	-	2,028	2,286	2,018	kWhe equiv
Capital Cost	$0.00	$1.41	$0.00	$0.00	$1.35	$1.41	$1.34	$M
Energy Cost	$7.15	$5.94	$7.38	$7.35	$6.16	$6.14	$6.07	$M
Demand Cost	$0.34	$0.24	$0.37	$0.34	$0.26	$0.24	$0.24	$M
PJM PLC Cost	$2.55	$1.31	$2.55	$2.55	$1.39	$1.31	$1.18	$M
Diesel Fuel Cost	$0.49	$0.49	$0.00	$0.00	$0.00	$0.00	$0.00	$M
Total Life Cycle Cost	$10.52	$9.54	$10.29	$10.23	$9.31	$9.25	$8.98	$M
Net Present Value	$0.00	$0.98	$0.22	$0.29	$1.21	$1.27	$1.53	$M
Break-even Cost Per Bus	$0	$0	$37,418	$47,968	$200,852	$210,968	$255,795	$/bus

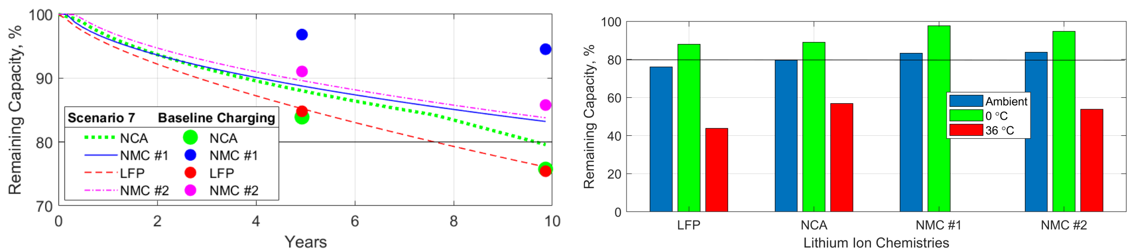

(a) Remaining capacity over time

(b) Remaining capacity after 10 years at different temperatures

Fig. 7: Impact of REopt based battery cycling profile in Scenario 7 on the life the battery

include the capital cost of EV buses, charging infrastructure and additional controls equipment required for smart-charging, VTB, and DR and wholesale market participation. Also, different use cases for fleet electrification such as package delivery vehicles will be evaluated.

Acknowledgement

This work was authored in part by the National Renewable Energy Laboratory, operated by Alliance for Sustainable Energy, LLC, for the U.S. Department of Energy (DOE) under Contract No. DE-AC36-08GO28308. Funding provided by the U.S. Department of Energy Office of Energy Efficiency and Renewable Energy and Eaton Corporation. The views expressed in the article do not necessarily represent the views of the DOE or the U.S. Government. The U.S. Government retains and the publisher, by accepting the article for publication, acknowledges that the U.S. Government retains a nonexclusive, paid-up, irrevocable, worldwide license to publish or reproduce the published form of this work, or allow others to do so, for U.S. Government purposes.

References

[1] L. Liu, A. Kotz, A. Salapaka, E. Miller, and W. F. Northrop, "Impact of time-varying passenger loading on conventional and electrified transit bus energy consumption," *Transportation Research Record*, vol. 0, no. 0, 2019.

[2] H.-Y. Liu, D. Dunea, S. Iordache, and A. Pohoata, "A review of airborne particulate matter effects on young childrens respiratory symptoms and diseases," *Atmosphere*, vol. 9, no. 4, 2018. [Online]. Available: https://www.mdpi.com/2073-4433/9/4/150

[3] D. Cutler, D. Olis, E. Elgqvist, X. Li, N. Laws, N. DiOrio, A. Walker, and K. Anderson, "Reopt: A platform for energy system integration and optimization," National Renewable Energy Laboratory, Tech. Rep. NREL/TP-7A40-70022, 2017, see also: https://reopt.nrel.gov/. [Online]. Available: https://www.nrel.gov/docs/fy17osti/70022.pdf

[4] M. Fries, M. Kerler, S. Rohr, M. Sinning, S. Schickram, M. Lienkamp, R. Kochhan, S. Fuchs, B. Reuter, P. Burda, and S. Matz, "An overview of costs for vehicle components, fuels, greenhouse gas emissions and total cost of ownership - update 2017," 08 2017.

[5] J. Vetter, P. Novk, M. Wagner, C. Veit, K.-C. Mller, J. Besenhard, M. Winter, M. Wohlfahrt-Mehrens, C. Vogler, and A. Hammouche, "Ageing mechanisms in lithium-ion batteries," *Journal of Power Sources*, vol. 147, no. 1, pp. 269 – 281, 2005.

[6] J. Cai, H. Zhang, and X. Jin, "Aging-aware predictive control of pv-battery assets in buildings," *Applied Energy*, vol. 236, pp. 478 – 488, 2019.

[7] A. Brooker, J. Gonder, L. Wang, E. Wood, and et. al, "Fastsim: A model to estimate vehicle efficiency, cost, and performance," Society of Automotive Engineers, Tech. Rep., 1 2015.

[8] DOE. (2018) Commercial reference buildings. [Online]. Available: https://www.energy.gov/eere/buildings/commercial-reference-buildings

[9] W. Longhi, "Schedule for electric service applicable in the entire territory," Rockland Electric Company, Tech. Rep. B.P.U. NO. 3 - Electricity Superseding P.U.C. NO. 2, 2010. [Online]. Available: https://www.oru.com/en/nj-rates-tariffs

[10] K. Smith, A. Saxon, M. Keyser, B. Lundstrom, Ziwei Cao, and A. Roc, "Life prediction model for grid-connected li-ion battery energy storage system," in *2017 American Control Conference (ACC)*, May 2017, pp. 4062–4068.

[11] S. Santhanagopalan, K. Smith, J. Naubauer, G.-H. Kim, A. Pesaran, and M. Keyser, *Design and Analysis of Large Lithium-Ion Battery Systems*. Boston, Massachusetts: Artech House, 2014.

[12] N. Oceanic and N. C. f. E. I. Atmospheric Administration. (2018) Climate data online. [Online]. Available: https://www.ncdc.noaa.gov/cdo-web/datatools/lcd